

# Pion-Photon Transition Form Factor and Pion Distribution Amplitude in QCD: Facing the Enigmatic Behavior of the BaBar Data

N. G. Stefanis<sup>a,b,\*</sup>, A. P. Bakulev<sup>a,\*\*</sup>, S. V. Mikhailov<sup>a</sup>, A. V. Pimikov<sup>a</sup>

<sup>a</sup>*Bogoliubov Laboratory of Theoretical Physics, JINR, 141980 Dubna, Russia*

<sup>b</sup>*Institut für Theoretische Physik II, Ruhr-Universität Bochum, D-44780 Bochum, Germany*

## Abstract

We present an extended analysis of the data for the pion-photon transition form factor from different experiments, CELLO, CLEO, and BaBar, and discuss various theoretical approaches which try to reason from them. We focus on the divergent behavior of the BaBar data for the pion and those for the  $\eta(\eta')$  pseudoscalar mesons and comment on recently proposed explanations for this discrepancy. We argue that it is not possible at present to accommodate these data within the standard QCD framework self-consistently.

**Keywords:** Meson transition form factors, pion distribution amplitude, QCD (light-cone) sum rules

## 1. Two-photon processes for $\pi^0$ and $\eta(\eta')$ in QCD

At the basis of applications of Quantum Chromodynamics (QCD), which governs the interactions of quarks and gluons, is the property of factorization of corresponding amplitudes in hard processes. Proving the property of factorization means that a hadronic process at large momentum transfer can be dissected in a product of distinct quantities each associated with separate regimes of dynamics. Then, subprocesses developing at short distances and involving partons—quarks and gluons—can be accurately described in a systematic way within perturbation theory. On the other hand, the dynamical (mainly nonperturbative) features of the hadron binding effects are encoded in correlators, which contain quark and gluon field operators, and can be parameterized in terms of light-cone wave functions and parton distribution functions. These quantities are process-independent and describe the universal interpolation between hadrons and their quark and gluon degrees of freedom as distributions over the fractions of

the longitudinal and intrinsic transverse momenta carried by the partons. They have to be determined by non-perturbative methods (models), lattice calculations, or from the data.

The (spacelike) transition form factors (TFFs) of pseudoscalar mesons, in particular the pion, have been extensively studied within QCD, because in leading order they are purely electromagnetic processes with the binding QCD effects being factorized out into the pion distribution amplitude (DA)—see [1] for a review and [2] for recent references. This means that for a highly virtual photon with the four-momentum transfer  $Q^2$  and a quasi-real photon with  $q^2 \rightarrow 0$ , the TFF can be cast as the convolution of the twist-two hard-scattering amplitude  $T(Q^2, q^2 \rightarrow 0, x) = Q^{-2}(1/x + O(\alpha_s))$ , describing the elementary process  $\gamma^*\gamma \rightarrow q\bar{q}$ , with the twist-two pion DA  $\varphi_\pi^{(2)}(x; \mu^2)$  so that

$$Q^2 F^{\gamma\gamma^*\pi}(Q^2) = \frac{\sqrt{2}}{3} f_\pi \int_0^1 Q^2 T(Q^2, x) \varphi_\pi^{(2)}(x; Q^2) dx + O\left(\frac{\delta^2}{Q^2}\right), \quad (1)$$

where  $\delta^2$  is the scale of the twist-four term taking val-

\*Corresponding author

\*\*Speaker of the talk at the “Psi-to-Phi” Conference

Email address: stefanis@tp2.ruhr-uni-bochum.de  
(N. G. Stefanis)

ues in the range  $\delta^2 = 0.15 \div 0.23 \text{ GeV}^2$ . Note that we have omitted for simplicity variables irrelevant for our discussion (see [3] and [4] for more details).

Several experimental groups have measured  $Q^2 F^{\gamma^* \gamma \pi^0}(Q^2, q^2 \rightarrow 0)$  and  $Q^2 F^{\gamma^* \gamma \eta(\eta')}(Q^2, q^2 \rightarrow 0)$  in two-photon processes  $e^+ e^- \rightarrow e^+ e^- \gamma^* \gamma \rightarrow e^+ e^- X$ , where  $X = \pi^0$  [5–7],  $\eta$  and  $\eta'$  [6, 8]. The range of probed photon momentum varies from  $0.7 \div 2.2 \text{ GeV}^2$  (CELLO), to  $1.64 \div 7.90 \text{ GeV}^2$  (CLEO), to  $4.24 \div 34.36 \text{ GeV}^2$  (BaBar). A recent compilation and discussion of the experimental data with the focus on the BaBar data can be found in [9]. The current situation from the experimental point of view can be summarized like this: all data for the TFFs pertaining to the non-strange part of the  $\eta$  and  $\eta'$  conform with the asymptotic QCD limit [3]  $\lim_{Q^2 \rightarrow \infty} Q^2 F^{\gamma^* \gamma \pi^0}(Q^2) \rightarrow \sqrt{2} f_\pi = 0.185$  and are best described by endpoint-suppressed DAs, while there is remarkable contrast to the high- $Q^2$  tail of the BaBar data for the  $\pi^0$  TFF [8, 9]. The rising trend of the BaBar data can be reproduced by the fit [7]  $Q^2 F(Q^2) = A(Q^2/10 \text{ GeV}^2)^\beta$  with  $A = 0.182 \pm 0.002 \text{ GeV}$  and  $\beta = 0.25 \pm 0.02$ . The latter value differs significantly from 0 predicted by QCD perturbation theory, cf. Eq. (1).

From the theoretical side, the conclusions drawn from different approaches are at odds with each other and cannot accommodate all available data simultaneously to resolve the puzzle. In our recent data analysis in [2] (see also [11]), we used Light-Cone Sum Rules (LCSRs) [12, 13] and performed an extended calculation of the pion TFF which takes into account the next-to-leading (NLO) order radiative corrections [14] and the twist-four contribution [12, 15], while also including in terms of uncertainties the main next-to-next-to-leading-order (NNLO) correction [4, 16] and the twist-six term, computed in [17]. The evolution of  $\varphi_\pi^{(2)}(x; \mu^2)$  with  $\mu^2 > 1 \text{ GeV}^2$  was also taken into account at the NLO level with  $\Lambda_{\text{QCD}}^{(3)} = 370 \text{ MeV}$  and  $\Lambda_{\text{QCD}}^{(4)} = 304 \text{ MeV}$ . The main observations are listed below.

(i) All data for  $Q^2 F^{\gamma^* \gamma \pi^0}(Q^2)$  in the range  $[1 \div 9] \text{ GeV}^2$  can be described at the level of  $\chi^2 < 1$  with only two Gegenbauer coefficients  $a_2$  and  $a_4$  with negative  $a_4$ , satisfying  $|a_4| \lesssim a_2$ .

(ii) The error ellipses of the data (CELLO, CLEO, BaBar) in the  $(a_2, a_4)$  plane overlap with the allowed region for these two parameters determined before [18] using QCD sum rules with nonlocal condensates [19]. These pion DAs are characterized by a strong suppression of their kinematical endpoints  $x = 0, 1$ , where  $x$  is the longitudinal momentum fraction of the quark inside the pion.

(iii) Beyond  $10 \text{ GeV}^2$ , an acceptable statistical description of the data ( $\chi^2 \geq 1$ ) demands the inclusion of a sizeable and positive Gegenbauer coefficient  $a_6$  with  $a_6 \simeq -1.8 a_4 \simeq 1.7 a_2$  (at the scale  $\mu_{\text{SY}} = 2.4 \text{ GeV}$  [10]). Still higher coefficients have been taken into account in [11] but found to have little effect. Moreover, it is difficult to select the optimal number of harmonics needed. Thus, the endpoint enhancement provided this way is not sufficient to reproduce the steep rise of the pion TFF observed by BaBar [7]. The range of variation of the associated pion DAs, conforming with this 3D  $(a_2, a_4, a_6)$  analysis, was worked out for both sets of data, i.e.,  $[1 \div 9] \text{ GeV}^2$  — set 1 and  $[1 \div 40] \text{ GeV}^2$  — set 2, in [11], see also Fig. 1. This figure shows best-fit results for both data sets in the form of bands of TFFs with errors stemming from the sum of the statistical errors and the twist-four uncertainties. The best-fit curve to set 1 in Fig. 1 is represented by the solid (blue) line, whereas the best-fit curve to set 2 at high  $Q^2$  is denoted by the dashed (red) line. This behavior makes it apparent that in the framework of LCSRs the fit to the BaBar data above  $9 \text{ GeV}^2$  deviates from that at low- $Q^2$  at the level of  $1\sigma$ .

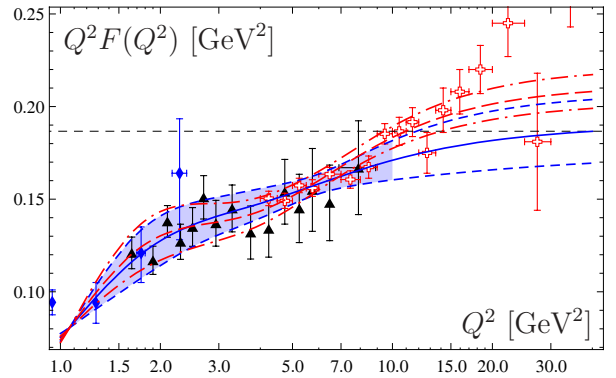


Figure 1: Best-fit curves to the experimental data for the TFF in the framework of LCSRs, inside corresponding bands of 68% CL regions as sums of statistical errors and twist-four uncertainties. Blue lines refer to set 1 and red lines to set 2 of the data from [5–7], with designations as in Fig. 2. The horizontal dashed line marks the asymptotic QCD limit.

Moreover, following [20] with some refinements explained in [2], one obtains the following windows for the values of the moments:  $\langle \xi^2 \rangle_\pi \in [0.23 \div 0.29]$ ,  $\langle \xi^4 \rangle_\pi \in [0.102 \div 0.122]$  and  $\langle \xi^2 \rangle_\pi \in [0.26 \div 0.29]$ ,  $\langle \xi^4 \rangle_\pi \in [0.11 \div 0.122]$ . These estimates were derived from our LCSR analysis [2, 11] by combining all data of set 1 with the lattice results obtained in [21] and [22], respectively. All values were evaluated at the typ-

ical lattice scale  $\mu_{\text{Lat}}^2 = 4 \text{ GeV}^2$ , using the definition  $\langle \xi^N \rangle_\pi \equiv \int_0^1 \varphi_\pi^{(2)}(x, \mu_{\text{Lat}}^2) (2x-1)^N dx$ , with  $\varphi_\pi^{(2)}(x, \mu^2)$  being normalized to unity. The “window” for  $\langle \xi^2 \rangle_\pi$ , obtained for the data with  $Q^2 < 10 \text{ GeV}^2$  (set 1), has in terms of the  $1\sigma$  error ellipse a large intersection with the most recent lattice estimates from [21–23]. Including into the fit the high- $Q^2$  BaBar data, this intersection significantly deteriorates—see [2, 11] for further details.

(iv) These findings indicate a significant discrepancy between the BaBar data for  $\pi^0$  and the method of LCSRs—and in more general terms the QCD factorization—at high- $Q^2$  values, an indication that the analysis in [17] is possibly no turning point in understanding the high- $Q^2$   $\pi^0$  BaBar data within QCD. Thus, our analysis does not confirm the opposite conclusions drawn in [17] which uses the same calculational scheme, but a larger value of the auxiliary Borel parameter  $M^2$ , notably  $1.5 \text{ GeV}^2$ , instead of values  $M^2 < 1 \text{ GeV}^2$  as in our approach, (which follows [12]) and more coefficients in the conformal expansion of the pion DA.

(v) Conformity with the increasing trend of the BaBar data can be actually achieved only with a flatlike pion DA, like that proposed in [24] and in a different context in [25]. However, the use of such a pion DA reduces the accuracy of the predicted TFF at lower values of  $Q^2$  [2, 26]. Moreover, it was emphasized in [2, 11, 27] that then one becomes unable to reproduce the BaBar data [8] for the nonstrange part of the  $\eta$ :  $|n\rangle = (1/\sqrt{2})(|u\bar{u}\rangle + |d\bar{d}\rangle)$ .<sup>1</sup> Indeed, employing the mixing scheme of [28], one can relate the TFF of  $|n\rangle$  to that of the  $\pi^0$  multiplied by a factor  $5/3$  due to the quark charges (also assuming that  $f_n = f_\pi$ ). Hence, it appears that the TFF for the  $\pi^0$  and the  $|n\rangle$  follow antithetic trends that correspond to DAs with distinct endpoint characteristics: extreme endpoint enhancement for the first vs. endpoint suppression for the second [27]. Because the properties of  $|n\rangle$  are not so sensitive to the choice of the mixing angle, such a strong antithetic behavior cannot be ascribed to this uncertainty. These results are shown in Fig. 2 using a logarithmic scale for  $Q^2$  and comparing them with all the available experimental data. Our predictions [2] are represented by a (green) strip whose width is a measure of the involved theoretical uncertainties, while the solid (blue) lines reproduce and extend farther out the predictions of [17]. The other lines will be explained shortly in Sec. 2. The crucial

question is: What kind of mechanism underlies such a strong flavor-symmetry breaking in the pseudoscalar meson sector of QCD?

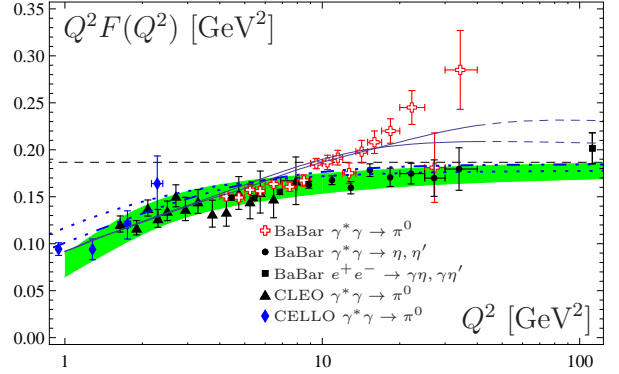


Figure 2: Theoretical predictions for the scaled transition form factors for  $\pi^0$  and the non-strange part of the  $\eta$  and  $\eta'$  from various theoretical approaches. The green strip contains the results obtained in [2] using the method described in the text. The two solid (blue) lines represent the findings of [17], whereas the dotted and the double-dotted-dashed lines denote two independent predictions derived from AdS/QCD in [29] and [30], respectively. The experimental data are taken from various experiments, referenced in the text.

In the next section, we will discuss some proposed explanations of the BaBar data without attempting to be comprehensive or conclusive.

## 2. Data Explanations

Let us start by recalling some facts related to the pion TFF. The CLEO data favor a pion DA close to the asymptotic (as) form [31, 32] excluding pion DAs of the Chernyak–Zhitnitsky (CZ) [33] type. Later, more detailed analyses of these data [10, 34] have excluded  $\varphi_\pi^{\text{CZ}}$  and  $\varphi_\pi^{\text{as}}$  at the  $4\sigma$  and the  $3\sigma$  level, respectively. To achieve an agreement with the CLEO data with  $1\sigma$  accuracy, one has to use endpoint-suppressed pion DAs of the form derived in [18] with the help of QCD sum rules with nonlocal condensates. In view of these findings, it was thought that more precise measurements which would extend the range of  $Q^2$  to much higher values, would confirm this trend because for large momentum transfers the application of perturbative QCD on the basis of collinear factorization should work better and better. Surprisingly, the rapid growth of the high- $Q^2$  BaBar data is at odds with these expectations, though this was not immediately recognized. But in coincidence with the publication of the BaBar data in the arXiv, two of us have clearly stated that no agreement between the stan-

<sup>1</sup>The separation of the nonstrange part of the  $\eta$  and the  $\eta'$  is model dependent. Moreover, the decay parameters  $f_\eta$  and  $f_{\eta'}$  are not well known and strongly depend on the mixing between the two eta mesons. We here employed the mixing scheme of Ref. [28].

standard QCD scheme and a rising TFF (scaled by  $Q^2$ ) can be achieved in terms of endpoint-vanishing  $\pi$  DAs [4].

Interestingly, other authors proposed at the same time explanations of such an “anomalous” behavior by appealing to flatlike pion DAs [24, 25, 35], outside the standard QCD context. Such approaches suffer from the point of view that they depend in a sensitive way on specific, i.e., *contextual* nonperturbative scales that cannot be linked to the standard QCD scales. Therefore, the meaning of these scales, with their particular values needed to explain the BaBar data, remains obscure. Consequently, though the BaBar data can be explained within such schemes, because they provide logarithmic enhancement to the TFF, it is not possible to identify a *single* underlying physical mechanism which yields enhancement of the pion TFF. Moreover, it is difficult to understand why the pion and the  $\eta$  should behave like “pointlike” particles (see, for instance, [36]) as implied by flatlike (or flat-top) DAs, while the DAs of the  $\eta'$  and the  $\eta_c$  should be close to their asymptotic forms (eventually with additional endpoint suppression).<sup>2</sup> The assertion in [35] that this is due to the larger mass of these particles is not very convincing, given that the DAs of the  $\pi^0$  and the  $\eta$  are very similar in shape in the nonlocal chiral quark model of [35], though the corresponding masses  $m_\pi = 140$  MeV and  $m_\eta = 548$  MeV are very different. Nevertheless, it would be premature to dismiss the correctness and/or relevance of such explanations.

The calculation of the  $\pi^0$ ,  $\eta$ , and  $\eta'$  TFFs has been carried out within holographic approaches of AdS/QCD, e.g., [29], [30], and [38]. In Fig. 2 the two broken (blue) lines represent the independent findings of two such approaches for  $Q^2 F^{\gamma^* \gamma \pi^0}(Q^2)$ . The dotted line denotes the prediction derived in [29], using a dressed electromagnetic current and taking into account the twist-two and the twist-four hadronic AdS components of the pion wave function (Eq. (43) in [29]) within a soft-wall holographic approach. The combination of the nonperturbative bound-state dynamics, predicted by the holographic AdS/QCD correspondence, with the perturbative Efremov–Radyushkin–Brodsky–Lepage evolution [3, 39] was treated in detail in [40]. The double-dotted-dashed line shows an analogous result [30], obtained by an extension of the hard-wall AdS/QCD model which includes the Chern–Simons term, required to reproduce the chiral anomaly of QCD. Note that the shown curve beyond 10 GeV<sup>2</sup> was generated by us. It is obvious that both displayed predictions are incongruent with the BaBar data for  $\pi^0$ , while they agree

with each other and with the BaBar data for the  $\eta(\eta')$ , though they somewhat overestimate all data at lower values of  $Q^2$ . Moreover, one observes that both predictions overlap with the band of the results derived in [2] and indicate conformity with endpoint-vanishing (or even endpoint-suppressed) pion DAs, like in the BMS formalism [18, 34].

The chiral anomaly plays an important role also in another approach, proposed in [41], which combines an exact nonperturbative sum rule, following from the dispersive representation of the axial anomaly, and quark-hadron duality. Within this approach it is claimed [42] that the increase of the BaBar data for the  $\pi^0$  is due to small corrections to the continuum (i.e., an infinite number of higher resonances) which entail a strong enhancement of the pion TFF, whereas the same effect for the  $\eta$  turns out to be several times smaller.<sup>3</sup> Depending on the particular mixing scheme adopted, the obtained predictions [41] for the  $\eta$  and  $\eta'$  mesons agree with the gross of the BaBar data for the associated TFFs. The usefulness of the dispersive approach [42]—which does not rely upon factorization—has to be further tested by extending it to the singlet channel. Another approach that relates the BaBar effect to the chiral anomaly is discussed in [43].

The light pseudoscalar meson-photon TFFs for the pion and the  $\eta$  and  $\eta'$  mesons were also discussed in [44], using a quark-flavor mixing scheme with only one mixing angle [45]. The associated DAs of these mesons are obtained from a light-cone wave function [46] by tuning a master parameter to appropriate values, whereas the constituent quark masses and the mixing angle play a relatively minor role. The main message from this analysis is that the (logarithmic) growth of the scaled TFF  $Q^2 F^{\gamma^* \gamma \pi^0}(Q^2)$ , indicated by the BaBar data, cannot be reproduced, while it remains unexplained why  $Q^2 F^{\gamma^* \gamma \pi^0}(Q^2)$  and  $Q^2 F^{\gamma^* \gamma \eta}(Q^2)$  should behave so differently. In fact, within the range of the model parameters, the BaBar data on  $Q^2 F^{\gamma^* \gamma \eta}(Q^2)$  and  $Q^2 F^{\gamma^* \gamma \eta'}(Q^2)$  can be explained simultaneously in the whole  $Q^2$  region. So far, no single mechanism with a physical interpretation within the standard QCD framework has been identified to explain the increase of the pion TFF as a result of particular quark-gluon interactions. Effects associated with the transverse-momentum degrees of freedom, intrinsic, i.e., inside the pion wave function, and resummed in terms of Sudakov factors, have also been discussed with respect to the BaBar data, see,

<sup>2</sup>Note parenthetically that the TFF for the  $\eta_c$  approaches the QCD prediction from below—see [37] for a discussion.

<sup>3</sup>Note that until now, all calculated corrections, perturbative and nonperturbative, amount in total to a negative contribution so that it is not clear how this scenario can be realized.



e.g., [37, 47, 48]. Some other examples of studies of the BaBar data in conjunction with particular nonperturbative QCD models can be found in [49–53].

### 3. Conclusions

The steep rise of the pion-photon TFF, observed by the BaBar Collaboration, indicates the existence of an enhancement mechanism that cannot be explained within the standard QCD scheme based on collinear factorization. This scheme predicts that at large values of the momentum transfer the pion does not rebound as a *unit* but reveals its partonic structure in such a way that the scaled TFF approaches a constant. Several theoretical approaches within QCD, like LCSR [2], Schwinger–Dyson equations [36], etc., are in conflict with the dichotomous behavior of the BaBar data for the TFFs of the pseudoscalar  $\pi^0$ ,  $\eta$ , and  $\eta'$  mesons. Should the anomalous behavior of the  $\pi^0$  BaBar data be confirmed by independent measurements, e.g., by the Belle experiment, then the BaBar effect will amount to crossing the Rubicon and the enigma will become a real challenge for QCD based on collinear factorization. Moreover, one would not be able to take recourse for an explanation to holographic models based on the AdS/QCD correspondence [29, 30, 40], because these are incompatible with the  $\pi^0$  BaBar data at high  $Q^2$ .

### 4. Acknowledgments

A. P. B. acknowledges the support from the Organizing Committee of the “Phi-to-Psi” Conference. A. V. P. wishes to thank for support the Ministry of Education and Science of the Russian Federation (projects No. 2.2.1.1/12360 and No. 2.1.1/10683). This work was supported in part by the Heisenberg–Landau Program under Grant 2011, the Russian Foundation for Fundamental Research (Grants No. 09-02-01149, 11-01-00182, and 12-02-00613), and the BRFBR–JINR Co-operation Program under contract No. F10D-002.

### References

- [1] S. J. Brodsky, G. P. Lepage, *Adv. Ser. Direct. High Energy Phys.* 5 (1989) 93.
- [2] A. P. Bakulev, S. V. Mikhailov, A. V. Pimikov, N. G. Stefanis, *Phys. Rev. D* 84 (2011) 034014.
- [3] G. P. Lepage, S. J. Brodsky, *Phys. Rev. D* 22 (1980) 2157.
- [4] S. V. Mikhailov, N. G. Stefanis, *Nucl. Phys. B* 821 (2009) 291.
- [5] H. J. Behrend, et al., *Z. Phys. C* 49 (1991) 401.
- [6] J. Gronberg, et al., *Phys. Rev. D* 57 (1998) 33.
- [7] B. Aubert, et al., *Phys. Rev. D* 80 (2009) 052002.
- [8] P. del Amo Sanchez, et al., *Phys. Rev. D* 84 (2011) 052001.
- [9] D. Muller, arXiv:1109.6610 [hep-ex].
- [10] A. Schmedding, O. Yakovlev, *Phys. Rev. D* 62 (2000) 116002.
- [11] A. P. Bakulev, S. V. Mikhailov, A. V. Pimikov, N. G. Stefanis, arXiv:1108.4344 [hep-ph].
- [12] A. Khodjamirian, *Eur. Phys. J. C* 6 (1999) 477.
- [13] I. I. Balitsky, V. M. Braun, A. V. Kolesnichenko, *Nucl. Phys. B* 312 (1989) 509.
- [14] F. del Aguila, M. K. Chase, *Nucl. Phys. B* 193 (1981) 517. E. Braaten, *Phys. Rev. D* 28 (1983) 524. E. P. Kadantseva, S. V. Mikhailov, A. V. Radyushkin, *Sov. J. Nucl. Phys.* 44 (1986) 326.
- [15] V. M. Braun, I. E. Filyanov, *Z. Phys. C* 44 (1989) 157.
- [16] B. Melić, D. Müller, K. Passek-Kumerički, *Phys. Rev. D* 68 (2003) 014013.
- [17] S. S. Agaev, V. M. Braun, N. Offen, F. A. Porkert, *Phys. Rev. D* 83 (2011) 054020.
- [18] A. P. Bakulev, S. V. Mikhailov, N. G. Stefanis, *Phys. Lett. B* 508 (2001) 279. *Phys. Lett. B* 590 (2004) 309, Erratum.
- [19] S. V. Mikhailov, A. V. Radyushkin, *Sov. J. Nucl. Phys.* 49 (1989) 494. *Phys. Rev. D* 45 (1992) 1754; A. P. Bakulev, S. V. Mikhailov, *Phys. Rev. D* 65 (2002) 114511.
- [20] N. G. Stefanis, *Nucl. Phys. Proc. Suppl.* 181–182 (2008) 199.
- [21] V. M. Braun, et al., *Phys. Rev. D* 74 (2006) 074501.
- [22] R. Arthur, et al., *Phys. Rev. D* 83 (2011) 074505.
- [23] M. A. Donnellan, et al., *PoS LAT2007* (2007) 369.
- [24] A. V. Radyushkin, *Phys. Rev. D* 80 (2009) 094009.
- [25] M. V. Polyakov, *JETP Lett.* 90 (2009) 228.
- [26] S. V. Mikhailov, N. G. Stefanis, *Mod. Phys. Lett. A* 24 (2009) 2858.
- [27] N. G. Stefanis, arXiv:1109.2718 [hep-ph].
- [28] T. Feldmann, P. Kroll, B. Stech, *Phys. Rev. D* 58 (1998) 114006.
- [29] S. J. Brodsky, F.-G. Cao, G. F. de Teramond, *Phys. Rev. D* 84 (2011) 0750012.
- [30] H. R. Grigoryan, A. V. Radyushkin, *Phys. Rev. D* 78 (2008) 115008.
- [31] P. Kroll, M. Raulfs, *Phys. Lett. B* 387 (1996) 848.
- [32] N. G. Stefanis, W. Schroers, H.-C. Kim, *Phys. Lett. B* 449 (1999) 299; *Eur. Phys. J. C* 18 (2000) 137.
- [33] V. L. Chernyak, A. R. Zhitnitsky, *Phys. Rept.* 112 (1984) 173.
- [34] A. P. Bakulev, S. V. Mikhailov, N. G. Stefanis, *Phys. Rev. D* 67 (2003) 074012; *Phys. Lett. B* 578 (2004) 91; *Phys. Rev. D* 73 (2006) 056002.
- [35] A. Dorokhov, arXiv:1109.3754 [hep-ph].
- [36] H. L. L. Roberts, C. D. Roberts, A. Bashir, L. X. Gutierrez-Guerrero, P. C. Tandy, *Phys. Rev. C* 82 (2010) 065202.
- [37] P. Kroll, arXiv:1109.5561 (2011).
- [38] A. Stoffers, I. Zahed, *Phys. Rev. C* 84 (2011) 025202.
- [39] A. V. Efremov, A. V. Radyushkin, *Phys. Lett. B* 94 (1980) 245.
- [40] S. J. Brodsky, F.-G. Cao, G. F. de Teramond, *Phys. Rev. D* 84 (2011) 033001.
- [41] Y. N. Klopov, A. G. Oganesian, O. V. Teryaev, *Phys. Rev. D* 84 (2011) 051901(R).
- [42] Y. N. Klopov, A. G. Oganesian, O. V. Teryaev, *Phys. Lett. B* 695 (2011) 130.
- [43] T. Pham, X. Pham, *Int. J. Mod. Phys. A* 26 (2011) 4125.
- [44] X.-G. Wu, T. Huang, *Phys. Rev. D* 84 (2011) 074011.
- [45] T. Feldmann, *Int. J. Mod. Phys. A* 15 (2000) 159.
- [46] X.-G. Wu, T. Huang, *Phys. Rev. D* 82 (2010) 034024.
- [47] H.-n. Li, S. Mishima, *Phys. Rev. D* 80 (2009) 074024.
- [48] Y. Bystritskiy, V. Bytev, E. Kuraev, A. Ilyichev, *Phys. Part. Nucl. Lett.* 8 (2011) 73.
- [49] P. Kotko, M. Praszalowicz, *Phys. Rev. D* 80 (2009) 074002.
- [50] E. R. Arriola, W. Broniowski, *Phys. Rev. D* 82 (2010) 094001.
- [51] S. Noguera, V. Vento, *Eur. Phys. J. A* 46 (2010) 197.
- [52] N. Kochelev, V. Vento, *Phys. Rev. D* 81 (2010) 034009.
- [53] S. Noguera, S. Scopetta, arXiv:1110.6402 [hep-ph].